

Ion mobility mass spectrometry of two tetrameric membrane protein complexes reveals compact structures and differences in stability and packing

Sheila C. Wang, Argyris Politis, Natalie Di Bartolo, Vassiliy N. Bavro, Stephen J. Tucker, Paula J. Booth, Nelson P. Barrera, Carol V. Robinson

Materials and Methods

BtuC₂D₂ Expression and Purification. BtuC₂D₂ was expressed and purified as reported previously.¹⁻² Briefly, BtuC₂D₂ was expressed from a pET-19b vector, with an N-terminal decaHis tag attached to the BtuC subunit, in *E. coli* cells. The protein was extracted from cell pellets in a lauryl dimethylamine *n*-oxide (LDAO) detergent by cell lysis and centrifugation; the cytosolic and LDAO-solubilised membrane fractions were applied to a Ni-NTA affinity column where the detergent was exchanged from LDAO to *n*-dodecyl- β -D-maltoside (DDM) detergent. The fractions were washed with 100 mM imidazole and BtuC₂D₂ was eluted in 500 mM imidazole. Further purification was carried out using gel filtration chromatography and BtuC₂D₂ was stored in 500 mM NaCl, 50 mM Tris pH 7.5, 0.1% DDM at -80°C.

KirBac3.1 Expression and Purification. KirBac3.1 gene from the α -proteobacterium *Magnetospirillum magnetotacticum* was codon optimised and synthesised *de novo* (GenScript, USA Inc), and cloned into the pET30a vector (Novagen), with a C-terminal 6xHis-tag. BL21 CodonPlus RP cells (Stratagene) were used for expression. Protein was purified as previously described,³ with the following modifications: cells were grown at 19°C overnight following induction and 50mM Tris-HCl pH7.8, 150mM NaCl, 50mM KCl was used as a lysis buffer. Protein sample was transferred into the following storage buffer (20 mM Tris pH 7.8, 100 mM NaCl, 10 mM KCl, 1 mM TriDM (*n*-tridecyl- β -D-maltopyranoside)) following a size-exclusion chromatography using S200 column (GE Pharmacia), and concentrated to approximately 5 mg/mL using Amicon Ultra (Millipore) ultrafiltration devices with 100kDa cut-off.

Ion Mobility-Mass Spectrometry. Ion mobility-mass spectrometry (IM-MS) measurements were carried out on a Synapt HDMS (Waters, Manchester, UK) quadrupole-

ion-trap-IM-MS instrument described in detail previously.⁴ Aliquots of complex-containing solutions (2 μ L of 5 μ M protein) in detergent (~ 200 μ M DDM or TriDM) and buffer (200 mM ammonium acetate, pH 7.6) were introduced via gold-coated nanoflow electrospray capillaries which were prepared as described previously.⁵ Instrument parameters were optimized to remove detergents while preserving noncovalent interactions between membrane protein subunits;^{1,6} typical MS conditions were: capillary voltage, 1.5 kV; cone voltage, 180-200 V; trap collision energy, 185-200 V; source temperature, 20°C; and backing pressure, 8 mBar.

The ion mobility separation cell contained N₂ at a pressure of 0.5 mBar and the traveling wave velocity was 250 ms⁻¹. Measurements were recorded at five wave heights (8, 8.5, 9, 9.5 and 10 V) to optimize IM separation. Data presented were acquired with a wave height of 10 V. Collision cross section (CCS) values reported are an average of the data recorded over all the wave heights. The CCS calibration procedure used is described previously.⁷ Briefly, drift-time measurements are normalized for charge state and an empirically derived, nonlinear correction function is applied to the drift times for calibrant ions such that their relative differences correspond to differences recorded for these ions by standard drift-tube techniques.⁷⁻¹³ Calibrations were then validated using known CCS data from other protein ions.¹⁴ The average relative precision of the measurements is approximately 4.4% and the average relative accuracy is approximately 12%, including errors associated with the calibrant cross-sections (up to 5%), the calibration curve (up to 5%), and the relative precision of replicate measurements (1.5%).

Modeling of the full length BtuC₂D₂ and KirBac3.1 tetramers. Both crystallized proteins (BtuC₂D₂, PDB code 1L7V;² KirBac3.1, PDB code 1XL6¹⁵) are incomplete; residues are missing in the N and C-terminal regions. The percentage of missing residues in BtuC, BtuD and KirBac3.1 correspond to 7.2%, 0.8% and 3.3% respectively. Models of full length BtuC₂D₂ and Kirbac3.1 were generated using the program Modeller.¹⁶ The final model structures were selected based on spatial restraints and DOPE assessment scores.¹⁷ Further optimization of the models using molecular dynamics and a conjugate gradient method was carried out as implemented in Modeller. For the full BtuC₂D₂ homology model, three X-ray crystal structures were used as templates. Modelling of the BtuC subunit was based on the structures 1L7V and 1S6J¹⁸ (structure 1S6J corresponds to the N-terminal region of the calcium regulatory domain from soybean calcium-dependent protein kinase alpha). The first

12 residues of the 1S6J structure have 100% identity with residues 12-23 in the BtuC subunit. Modelling of the BtuD subunit was based on the 2QI9¹⁹ structure (which corresponds to the BtuC₂D₂ assembly complexed with BtuF). Modelling of the full length KirBac3.1 structure employed only the crystal structure PDB file 1XL6 as a template. Protein structures in all figures were generated in PyMOL.

Theoretical CCS calculations. The CCSs for full-length BtuC₂D₂ and KirBac3.1 were calculated using the projection approximation (PA) employed in the MOBCAL program,²⁰⁻²¹. A range of theoretical CCSs for the BtuC₂D₂ tetramer based on models with collapsed (6495 Å²) or fully extended (6702 Å²) N-termini tails. This program has been adapted for either all-atom coordinate sets or coarse-grained models.⁷ In all cases, the projection approximation values are reported as an estimated CCS of the model structures.

Modeling of KirBac3.1 and BtuCD₂ trimers. To investigate the topologies of the BtuCD₂ and Kirbac3.1 trimers observed experimentally, we start from the full length models of the tetramers. For BtuCD₂ we remove one C subunit from the corresponding tetramer. The theoretical CCS is then calculated for the remaining atoms using MOBCAL.²⁰⁻²¹ The calculated CCS are ~17% larger than the experimental CCSs, which suggests that BtuCD₂ undergoes significant structural rearrangements in the gas phase. We therefore collapse the N-terminal tail of the BtuC subunit using molecular modelling tools as implemented in visual molecular dynamics (VMD),²² and then rotate it so that the BtuC subunit contacts both BtuD subunits. The CCS for this conformation agrees well with experimental values. We subsequently unfold the C-terminal domain of one BtuC subunit by 7%. For the KirBac3.1 trimer, removal of one monomer from the tetramer and subsequent rotations of the remaining trimers reduces the 4-fold symmetry of the initial tetrameric assembly to a 3-fold symmetric trimer. A collapsed assembly is generated by first folding the N- and C-termini of all three subunits and then rotating and translating the cytoplasmic domain towards the transmembrane region. All model structures were energy minimized, using NAMD²³ to eliminate possible steric clashes and to ensure energetically favourable conformations.

Table S1. Structural properties of the KirBac3.1 and BtuC₂D₂ tetramers.

	KirBac3.1	BtuC₂D₂
Number of residues	1204	1196
Number and type of subunits	Homotetramer (4 transmembrane subunits)	Heterotetramer (2 transmembrane and 2 soluble subunits)
Number of residues in the N- and C-termini tails	34 (N-terminus tail) 32 (C-terminus tail)	24 (N-terminus tail of BtuC)
MW measured (tetramer)	134960 ± 48 Da	129900.6 ± 16 Da
MW calculated (tetramer)	134951.2 Da	129654.6 Da
MW measured (trimer)	101261.9 ± 92 Da	92117.4 ± 8 Da (BtuCD ₂)
MW calculated (trimer)	101213.4 Da	91938.5 Da (BtuCD ₂)
MW measured (monomer)	33751.6 ± 24 Da	37771.8 ± 27 Da (BtuC)
MW calculated (monomer)	33737.8 Da	37716.4 (BtuC)
MW Transmembrane region	39236.5 Da	66285.7 Da
MW Soluble (cytoplasmic and periplasmic) region	95714.6 Da	63368.9 Da
Z average	25.3	21.2
Activation energy coefficient*	46	35
Number of solvent-exposed R,H,K residues total**	27	26
Number of solvent-exposed R,H,K residues in the transmembrane region	0	4
Number of solvent-exposed R,H,K residues in the soluble region	27	22
ASA total [#]	58813 Å ²	52550 Å ²
ASA transmembrane region	10634 Å ²	15561 Å ²
ASA soluble region	48179 Å ²	36989 Å ²
Molecular volume total [§]	182005 Å ³	169886 Å ³
Molecular volume transmembrane region	45727 Å ³	51379 Å ³
Molecular volume soluble region	136278 Å ³	118507 Å ³
CCS experimental (tetramer) [‡]	6900 ± 700 Å ²	6600 ± 700 Å ²
CCS calculated (tetramer)	6969 Å ²	6495 – 6702 Å ² based on models with collapsed (6495 Å ²) or fully extended (6702 Å ²) BtuC N-terminal tails. An intermediate of 6579 Å ² is quoted in the main text.
CCS calculated (trimer)	4561 Å ² (collapsed trimer) 5868 Å ² (3-fold symmetric with collapsed N and C termini)	4362 Å ² (BtuCD ₂ with a compact subunit arrangement) 4501 Å ² (BtuCD ₂ with partial unfolding of BtuC) 4762 Å ² (BtuCD ₂ derived from tetramer with collapsed BtuC N-termini)
CCS calculated (monomer)	2937 Å ²	2650 Å ² (BtuC)

* The activation energy coefficient (minimal energy required to detect the intact membrane protein) was calculated according to the following equation:⁶

Activation energy coefficient = z average × [(cone voltage/200V) + (trapCE voltage/240V)]; 200 and 240V correspond to the maximal Synapt instrumental voltages for the cone and trap CE respectively. For KirBac3.1, 200V cone and 200V trapCE were used whereas for BtuC₂D₂ 180V cone and 185V trapCE were used.

** Solvent accessibility is calculated based on an accessible surface area (ASA) greater than 150 Å². In Figure S1, the positions of the most solvent exposed R, H, K residues are shown.

[#] ASA was calculated using Gerstein's program.²⁴

[§] Molecular volume was calculated using the polyhedra volume approximation.²⁵

[‡]The measured CCSs do not vary significantly between the 21+ to 23+ ions of KirBac3.1 and the 19+ to 21+ ions of BtuC₂D₂, therefore the values reported are an average across these charge state distributions.

Table S2. Structural properties of the subunit-subunit interfaces in the KirBac3.1 and BtuC₂D₂ tetramers.

	KirBac3.1	BtuC₂D₂
Number and type of interfaces*	4 identical subunit-subunit interfaces	1 BtuC-BtuC interface, 1 BtuD-BtuD interface and 2 identical BtuC-BtuD interfaces
<i>Interfaces disrupted upon removal of one KirBac3.1 subunit</i>		
Number of residues	250	
Number of R, H, K residues in the soluble region	32	
Number of R, H, K residues in the transmembrane region	8	
ASA total	10376.9 Å ²	
Molecular volume	44991.1 Å ³	
<i>Interfaces disrupted upon removal of one BtuC subunit</i>		
Number of residues		129
Number of R, H, K residues in the soluble region		10
Number of R, H, K residues in the transmembrane region		9
ASA total		5307 Å ²
Molecular volume		22233 Å ³
<i>Interfaces disrupted upon removal of one BtuD subunit</i>		
Number of residues		122
Number of R, H, K residues in the soluble region		17
Number of R, H, K residues in the transmembrane region		3
ASA total		4845 Å ²
Molecular volume		21933 Å ³

* Interfaces are defined as residues which have an ASA decreasing by $> 1 \text{ Å}^2$ in the presence of two interacting subunits. The Protorp server was used. (<http://www.bioinformatics.sussex.ac.uk/protorp>)²⁶

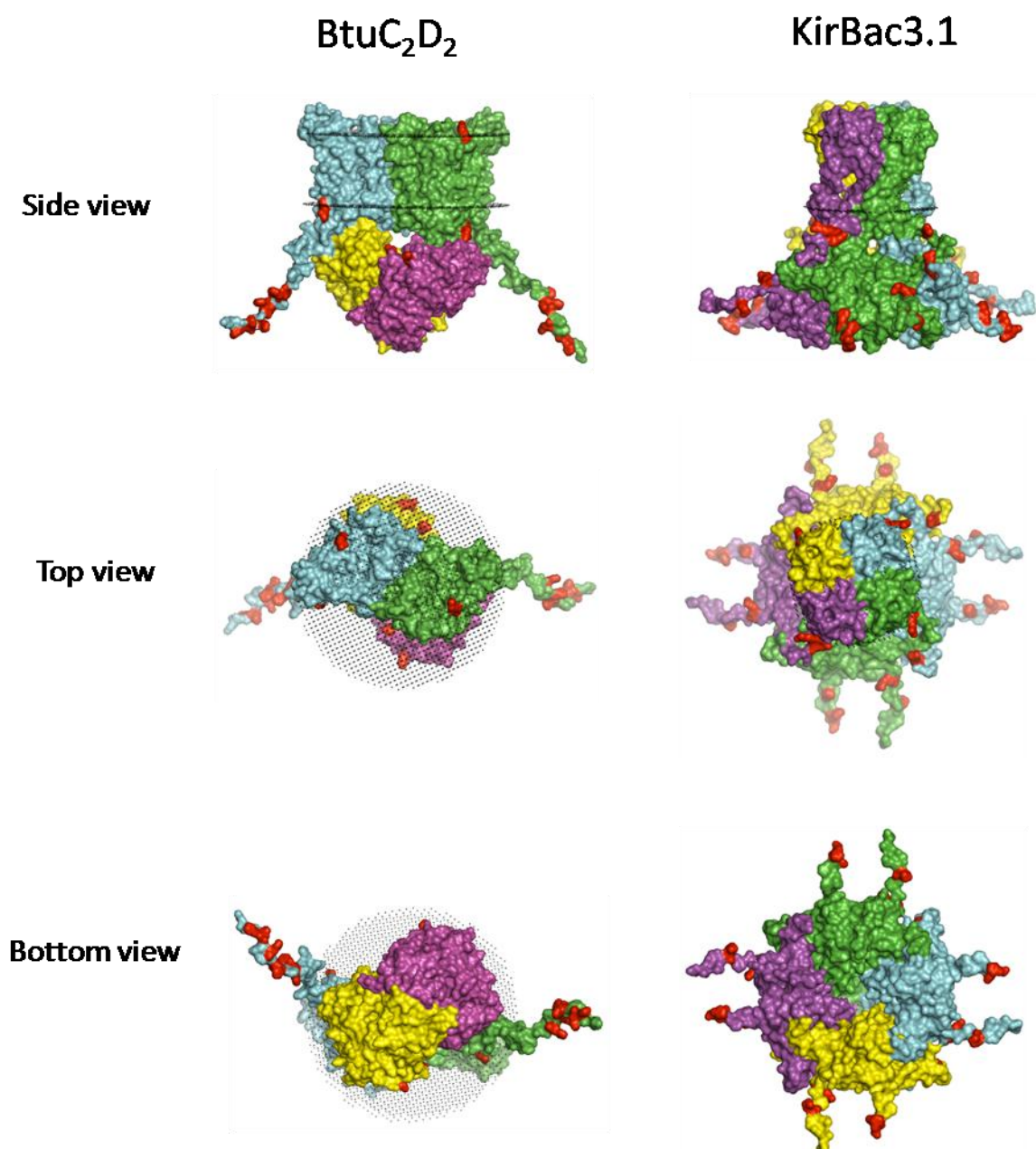


Figure S1. The most solvent-exposed basic residues identified on the soluble domains of BtuC₂D₂ and KirBac3.1 tetramers. Basic residues within the soluble regions are selected based on an accessible surface area larger than 150 Å² (red residues). For the BtuC₂D₂ and KirBac3.1 tetramers, 22 and 27 basic residues respectively were identified. Black planes indicate the hydrophobic boundaries of the transmembrane regions.²⁷

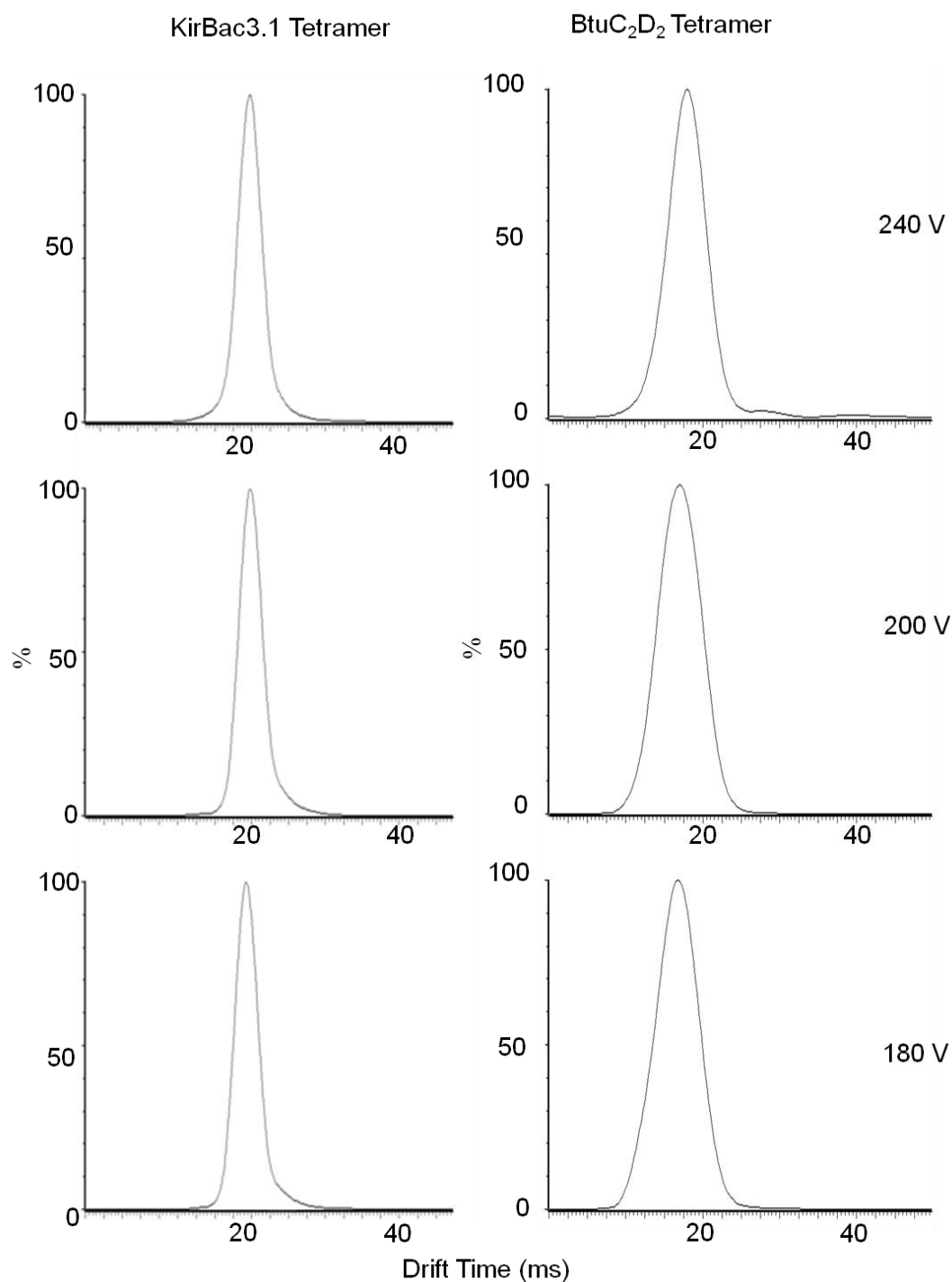
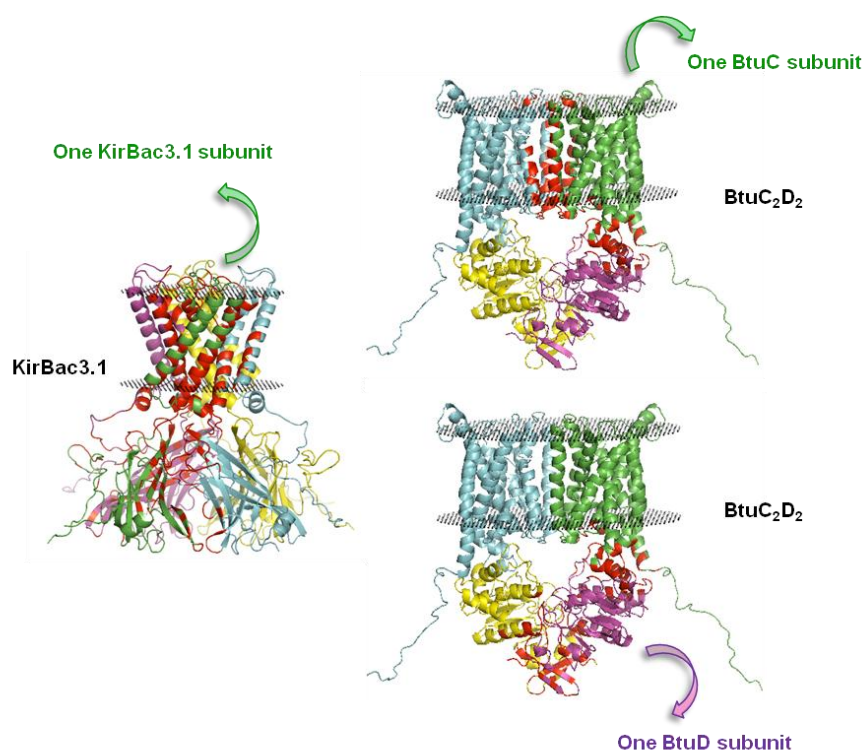


Figure S2. Arrival-time distributions for ions at m/z values corresponding to the 21+ of the KirBac3.1 tetramer and to the 21+ ions of the BtuC₂D₂ tetramer acquired at accelerations of 180, 200 and 240V in the trap region of the instrument. The mobility resolution of the arrival time distributions of the charge states of the KirBac3.1 and BtuC₂D₂ tetramers are typically 6-10 $t/\Delta t$ and 2-4 $t/\Delta t$ respectively. The arrival time distributions of the KirBac3.1 and BtuC₂D₂ tetramers are relatively insensitive to increasing activation energies.

A



B

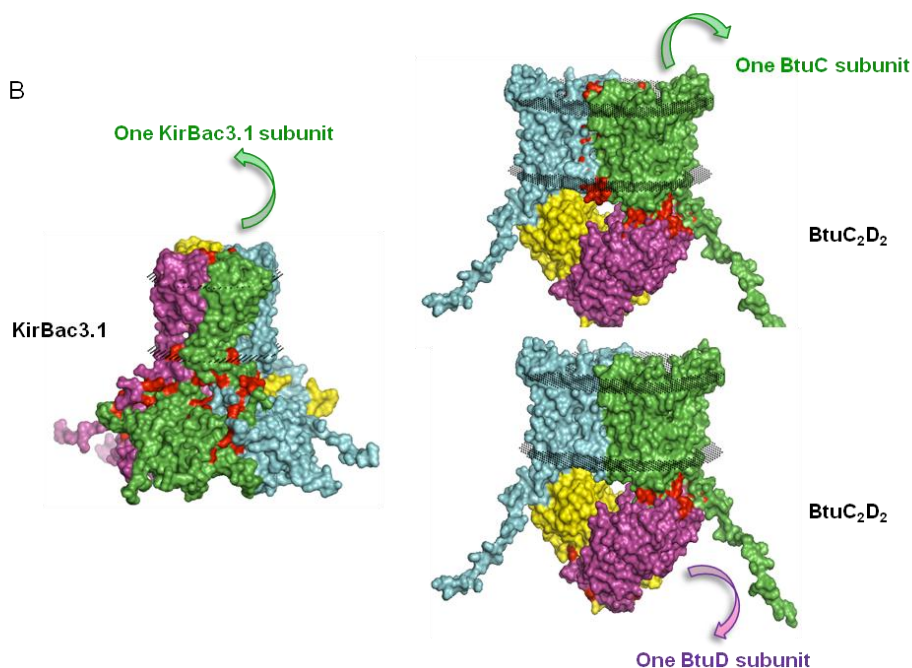


Figure S3. Subunit-subunit interfaces in the KirBac3.1 and BtuC₂D₂ tetramers.

A. Residues located within the subunit interfaces are coloured in red. These subunit interfaces are disrupted upon removal of one monomer as indicated. Each monomer is drawn in a different colour. The removal of one KirBac3.1 monomer affects a larger interfacial area than the removal of either one BtuC or one BtuD subunit. **B.** All basic residues identified within the subunit interfaces are coloured in red. Black planes indicate the hydrophobic boundaries of the transmembrane regions.²⁷

References

- (1) Barrera, N. P.; Di Bartolo, N.; Booth, P. J.; Robinson, C. V. *Science* **2008**, *321*, 243.
- (2) Locher, K. P.; Lee, A. T.; Rees, D. C. *Science* **2002**, *296*, 1091.
- (3) Kuo, A.; Domene, C.; Johnson, L. N.; Doyle, D. A.; VÃ©nien-Bryan, C. *Structure* **2005**, *13*, 1463.
- (4) Pringle, S. D.; Giles, K.; Wildgoose, J. L.; Williams, J. P.; Slade, S. E.; Thalassinou, K.; Bateman, R. H.; Bowers, M. T.; Scrivens, J. H. *International Journal of Mass Spectrometry* **2007**, *261*, 1.
- (5) HernÃ¡ndez, H.; Robinson, C. V. *Nature Protocols* **2007**, *2*, 715.
- (6) Barrera, N. P.; Isaacson, S. C.; Zhou, M.; Bavro, V. N.; Welch, A.; Schaedler, T. A.; Seeger, M. A.; Miguel, R. N.; Korkhov, V. M.; van Veen, H. W.; Venter, H.; Walmsley, A. R.; Tate, C. G.; Robinson, C. V. *Nature Methods* **2009**, *6*, 585.
- (7) Ruotolo, B. T.; Benesch, J. L. P.; Sandercock, A. M.; Hyung, S. J.; Robinson, C. V. *Nature Protocols* **2008**, *3*, 1139.
- (8) Lorenzen, K.; Olia, A. S.; Uetrecht, C.; Cingolani, G.; Heck, A. J. R. *Journal of Molecular Biology* **2008**, *379*, 385.
- (9) Scarff, C. A.; Patel, V. J.; Thalassinou, K.; Scrivens, J. H. *Journal of the American Society for Mass Spectrometry* **2009**, *20*, 625.
- (10) Shvartsburg, A. A.; Smith, R. D. *Analytical Chemistry* **2008**, *80*, 9689.
- (11) Thalassinou, K.; Grabenauer, M.; Slade, S. E.; Hilton, G. R.; Bowers, M. T.; Scrivens, J. H. *Analytical Chemistry* **2009**, *81*, 248.
- (12) Uetrecht, C.; Versluis, C.; Watts, N. R.; Wingfield, P. T.; Steven, A. C.; Heck, A. J. R. *Angewandte Chemie - International Edition* **2008**, *47*, 6247.
- (13) Williams, J. P.; Giles, K.; Green, B. N.; Scrivens, J. H.; Bateman, R. H. *Rapid Communications in Mass Spectrometry* **2008**, *22*, 3179.
- (14) Clemmer, D. E. *Clemmer collision cross-section database* **2008**.
- (15) Gulbis, J. M.; Kuo, A.; Smith, B.; Doyle, D. A.; Edwards, A.; Arrowsmith, C.; Sundstrom, M. *Two Intermediate Gating State Crystal Structures of the KirBac3.1 K Channel+* **2005**.
- (16) Sali, A.; Blundell, T. L. *Journal of Molecular Biology* **1993**, *234*, 779.
- (17) Shen, M. Y.; Sali, A. *Protein Science* **2006**, *15*, 2507.
- (18) Weljie, A. M.; GagnÃ©, S. M.; Vogel, H. J. *Biochemistry* **2004**, *43*, 15131.
- (19) Hvorup, R. N.; Goetz, B. A.; Niederer, M.; Hollenstein, K.; Perozo, E.; Locher, K. P. *Science* **2007**, *317*, 1387.
- (20) Mesleh, M. F.; Hunter, J. M.; Shvartsburg, A. A.; Schatz, G. C.; Jarrold, M. F. *Journal of Physical Chemistry* **1996**, *100*, 16082.
- (21) Shvartsburg, A. A.; Jarrold, M. F. *Chemical Physics Letters* **1996**, *261*, 86.
- (22) Humphrey, W.; Dalke, A.; Schulten, K. *Journal of Molecular Graphics* **1996**, *14*, 33.
- (23) Phillips, J. C.; Braun, R.; Wang, W.; Gumbart, J.; Tajkhorshid, E.; Villa, E.; Chipot, C.; Skeel, R. D.; KalÃ©, L.; Schulten, K. *Journal of Computational Chemistry* **2005**, *26*, 1781.
- (24) Gerstein, M. *Acta Crystallog. Sect. A* **1992**, *48*, 271.
- (25) Voss, N. R.; Gerstein, M. *Journal of Molecular Biology* **2005**, *346*, 477.
- (26) Reynolds, C.; Damerell, D.; Jones, S. *Bioinformatics* **2009**, *25*, 413.
- (27) Lomize, A. L.; Pogozheva, I. D.; Lomize, M. A.; Mosberg, H. I. *Protein Science* **2006**, *15*, 1318.